

Rapid Communications

Rapid Communications are intended for the accelerated publication of important new results and are therefore given priority treatment both in the editorial office and in production. A Rapid Communication in Physical Review B should be no longer than four printed pages and must be accompanied by an abstract. Page proofs are sent to authors.

Angular dependence of specular resonant nuclear scattering of x rays

A. Q. R. Baron, J. Arthur, and S. L. Ruby

Stanford Linear Accelerator Center, Stanford Synchrotron Radiation Laboratory, P.O. Box 4349, Stanford, California 94309

A. I. Chumakov and G. V. Smirnov

Russian Research Center, "Kurchatov Institute," 123182 Moscow, Russia

G. S. Brown

Department of Physics, University of California at Santa Cruz, Santa Cruz, California 95064

(Received 28 March 1994)

Specular scattering of x rays by electrons in a material becomes large at grazing angles below the critical angle for external reflection. In contrast, we observe specular scattering by resonant nuclei to peak at the critical angle and decrease at smaller angles. This is the result of the influence of the electronic scattering on the nuclear response of the system and is explained using an optical model. A distorted-wave Born approximation shows the specular nuclear signal should be large at angles where the electronic reflectivity varies rapidly with angle.

Synchrotron radiation studies of resonant nuclear systems¹ combine the inherent collimation of a synchrotron source with the sensitivity of the nuclear resonance to its atomic environment. Thus, there is tremendous potential for these experiments to provide both the structural information that accompanies a well-defined photon momentum, and the chemical, magnetic, and motional information of resonant nuclear (Mössbauer) studies. In particular, the conventional (electronic) x-ray scattering techniques used to investigate thin films and surfaces may be applied to resonant nuclear systems. These techniques frequently employ a grazing incidence geometry which increases the path length of x rays in a thin sample and permits use of total external reflection^{2,3} and related phenomena^{4,5} that occur because the index of refraction for materials at x-ray frequencies is less than one. In fact, the change in penetration depth with grazing angle has been applied in some Mössbauer studies of thin layers using highly collimated radioactive sources.⁶⁻⁸ Here we describe an interesting effect observed at grazing incidence in synchrotron Mössbauer experiments.

Synchrotron resonant nuclear scattering experiments are unique in that they allow resonant scattering events to be separated from nonresonant ones by gating in time. The synchrotron provides a short pulse⁹ of x rays so the scattering may be divided into prompt and delayed events. If the photon arrival time at the detector is delayed (relative to the transit time through vacuum) then it must have interacted resonantly with the sample. Furthermore, in a kinematic limit, any nonresonant interaction leads to instantaneous scattering, so gating in time permits resonant processes to be

separated from nonresonant ones. However, in the dynamical system discussed here, the nonresonant scattering strongly influences the angular dependence of the delayed scattering. This has not been observed previously because most synchrotron resonant nuclear scattering experiments have used electronically forbidden (pure nuclear) Bragg reflections, largely to reduce the background of nonresonantly scattered x rays. Improvements in optics¹⁰⁻¹² and detectors^{13,14} now allow experiments to be done in the presence of large background from electronic scattering, both in a Bragg geometry¹⁵ and near the region of total external reflection.^{16,17} Thus, it is possible to study a much wider variety of samples, in particular thin films and surfaces. However, the effects of strong electronic scattering into the reflected beam must be recognized.

We consider the effect of the electronic scattering on the delayed component of the specular (or coherent) scattering from a thin layer of ⁵⁷Fe. This may be thought of as a simple prototype for future investigation of thin films and surfaces. We observe the delayed or resonant signal from a sample with strong electronic scattering is maximized at angles where the nonresonant scattering varies rapidly with angle, or, in the case of grazing incidence, at the critical angle.

Like the other grazing incidence phenomena mentioned above, this one may be understood using a simple optical model. The reflected amplitude for x rays incident on a planar vacuum-material interface at grazing angle θ is described by the Fresnel (amplitude) reflection coefficient¹⁸

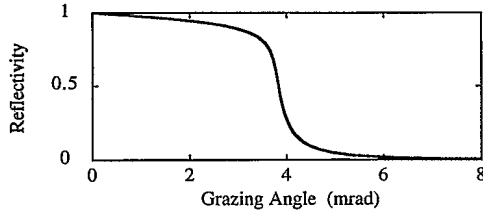


FIG. 1. Specular reflectivity of iron for 14.4 keV x rays.

$$R_\theta = \frac{1 - \beta}{1 + \beta}, \quad (1)$$

where $\beta \equiv [1 - 2\delta/\theta^2]^{1/2}$ and δ is the complex decrement of the index of refraction of the material from one, $\delta = 1 - n$. The reflectivity, $|R_\theta|^2$, is shown in Fig. 1 for a material with $\delta = \delta_e = (7.4 \times 10^{-6}) + (3.4 \times 10^{-7})i$, appropriate for bulk density iron and 14.4 keV x rays.¹⁹ The reflectivity saturates at angles below the critical angle, $\theta_c = (2 \operatorname{Re}\{\delta_e\})^{1/2}$, at 3.8 mrad.

The effect of the nuclear resonance is included by adding a frequency-dependent nuclear contribution to δ . Taking $\delta = \delta(\omega) = \delta_e + \delta_n(\omega)$, R_θ becomes $R_\theta(\omega)$. For an isolated resonance, the nuclear contribution δ_n has a complex Lorentzian frequency dependence, $\delta_n(\omega) \propto [\hbar(\omega - \omega_0) - i\Gamma/2]^{-1}$, where ω_0 is the resonance frequency and Γ is the linewidth ($\Gamma = 4.7 \times 10^{-9}$ eV and $\hbar\omega_0 = 14.4$ keV in ⁵⁷Fe). More generally, δ_n is a sum over all the hyperfine components of a transition, with appropriate weighting for their angular momenta and the photon polarization.

The time response to an impulse excitation is the Fourier transform of the frequency response. Therefore, the delayed response of a system should be related to the frequency varying part of the reflectivity; any frequency-independent contribution appears in the impulse response only at $t=0$. Mathematically, the impulse response is

$$G_\theta(t) = (2\pi)^{-1} \int_{-\infty}^{+\infty} R_\theta(\omega) e^{i\omega t} d\omega. \quad (2)$$

The (integrated) delayed intensity after pulse excitation at $t=0$ is proportional to

$$I_\theta = \int_{0^+}^{+\infty} |G_\theta(t)|^2 dt, \quad (3)$$

where 0^+ indicates the limit is to be taken from positive times. We write $R_\theta(\omega) = R_\theta^e + R'_\theta(\omega)$, where R_θ^e is the reflectivity for frequencies far from the nuclear resonance frequency (the electronic reflectivity in the absence of nuclei) and $R'_\theta(\omega)$ is a frequency-dependent part which goes to zero at large frequencies. Inserting this into Eq. (2), the R_θ^e term is seen to have a δ -function dependence on time so that it drops out of Eq. (3) because of the 0^+ integration limit. Since $G(t)$ is causal [$G(t < 0) = 0$], Parseval's theorem gives

$$I_\theta = (2\pi)^{-1} \int_{-\infty}^{+\infty} |R_\theta(\omega) - R_\theta^e|^2 d\omega. \quad (4)$$

At large angles [$\theta^2 \gg 2|\delta(\omega)|$], the scattering is kinematic and $R_\theta(\omega)$ separates into a sum of two terms: one corre-

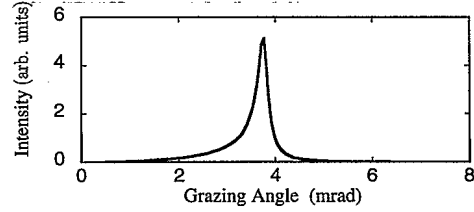


FIG. 2. Delayed intensity specularly reflected by a material with a single nuclear transition. Calculated from Eq. (4) using $\delta = \delta_e = (7.4 \times 10^{-6}) + (3.4 \times 10^{-7})i$, $\delta_n(\omega_0) = 10^{-5}i$, and $\Gamma = 4.7 \times 10^{-9}$ eV.

sponding to scattering by nuclei without electrons present and one for scattering by electrons without nuclei present. The electronic part drops out of Eq. (4) so the delayed signal decouples from all electronic scattering. This demonstrates the earlier statement that resonant interactions may be separated from nonresonant interactions in kinematic time domain experiments.

In regions of high reflectivity, such as near the electronic critical angle, separation into a sum of a nuclear part and an electronic part is not possible, but one may numerically integrate Eq. (4) to give the result shown in Fig. 2. The delayed reflectivity peaks at the electronic critical angle.²⁰ This follows from Eq. (4): the delayed reflectivity will be high when the magnitude of the difference, $|R_\theta(\omega) - R_\theta^e|$, is large over an appreciable frequency range. Since $R_\theta(\omega)$ depends on frequency only through the parameter $\delta(\omega)/\theta^2$, one would expect the difference to be most sensitive to changes in frequency at angles where R_θ^e is most sensitive to changes in angle. More formally, expansion to first order in $\delta_n(\omega)/\delta_e$ (the validity of this expansion will be discussed below) gives

$$R_\theta(\omega) - R_\theta^e \approx -\frac{\theta}{2\delta_e} \frac{dR_\theta^e}{d\theta} \delta_n(\omega), \quad (5)$$

which explicitly shows the dependence on the derivative of the electronic reflectivity with angle. The separation of the frequency and angular dependence means it is reasonable to think of the integral in Eq. (4), the delayed intensity, as being large where there is a fast change in the electronic reflectivity with angle (i.e., at the critical angle). Note that in the case of Bragg diffraction from a perfect crystal, the formula analogous to Eq. (5) also goes as $dR_\theta^e/d\theta$.

Evaluation of the derivative in Eq. (5) gives

$$\begin{aligned} R_\theta(\omega) - R_\theta^e &\approx \frac{2}{1 + \beta_e} \frac{2\beta_e}{1 + \beta_e} \frac{\delta_n(\omega)}{2\theta^2 \beta_e^2} \\ &= T_\theta^e T_\theta'^e \tilde{R}(\omega), \end{aligned} \quad (6)$$

where $\beta_e = [1 - 2\delta_e/\theta^2]^{1/2}$, $T^e = 2/(1 + \beta_e)$ is the (Fresnel) amplitude transmission coefficient into the electronic solid (without nuclei present), and $T'^e = 2\beta_e/(1 + \beta_e)$ is the transmission back out. $\tilde{R} = \delta_n/2\theta^2 \beta_e^2$ is the reflection coefficient for an interface between the electronic material, index $1 - \delta_e$, and a material with index of refraction $1 - \delta_e - \delta_n(\omega)$. \tilde{R} has the characteristic $1/q^2$ amplitude dependence ($1/q^4$ intensity) of kinematic small-angle scattering, where q is the momentum transfer in the material

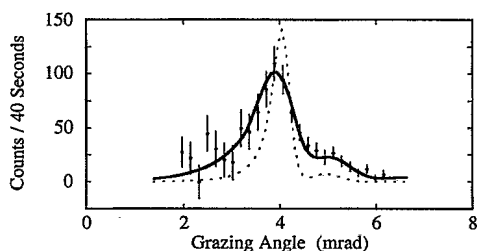


FIG. 3. Measured delayed intensity reflected from a thin layer of ^{57}Fe (points). The solid line is a calculation based on the full theory while the dashed line is a first-order calculation.

($q \propto \theta\beta_e = [\theta^2 - 2\delta]^{1/2}$). This quickly reduces the coherent scattering at higher angles. Below the critical angle, the intensity is reduced both due to the reduced transmission into the material (T^e becomes small) and due to the fact that q in \bar{R} becomes large, though imaginary (the extinction of the wave field due to electronic scattering reduces the illumination of the nuclei).

Investigation of Eq. (6) shows it to be a distorted-wave Born approximation.²¹ It explicitly includes multiple electronic scattering, which generates the distorted wave, and the nuclear scattering is added in a kinematic limit. This is different than the fully kinematic situation, mentioned above, where the electronic and nuclear scattering are both small and decouple so that the delayed scattering is not at all influenced by the nonresonant interaction. In this distorted-wave approximation, the amount of nuclear scattering is dependent on the electronic scattering, but the shape of the impulse response is not affected since Eq. (6) is linear in $\delta_n(\omega)$. Inclusion of terms of higher order in $\delta_n(\omega)$ would lead to changes in the time response.

Figure 3 shows the delayed intensity reflected from a 240 Å film of 95% enriched ^{57}Fe deposited on a smooth glass substrate. The solid line is a dynamical calculation carried out to all orders in δ_n . It is based on a recursive optical approach for layered structures²² and uses a carefully developed model of the layer. The slight tail of the delayed reflectivity at higher angles results from the layered nature of the sample and is analogous to the Kiessig interference fringes observed in electronic x-ray scattering from thin films.²³ The rounding of the peak, relative to Fig. 2, arises due to the fact that integration of delayed intensity began at $t=4$ ns after the synchrotron pulse, not the limiting $t=0^+$ used in Eq. (4).

It remains to comment on the validity of the first-order approximation used in Eqs. (5) and (6). For the enriched sample used here, $|\delta_n(\omega)| \sim |\delta_e|$ for frequencies near resonance. Therefore, although the first-order discussion is useful for qualitative understanding, it is necessary to go to higher orders to obtain good quantitative agreement. This is illustrated by the dashed line in Fig. 3, which is calculated to first order in δ_n . The peak in this calculation is both shifted from the data²⁴ and much narrower.

Effects due to higher-order terms may be expected to fall into two broad categories: those due to multiple nuclear scattering and those that may result from having both dynamical nuclear and dynamical electronic scattering in the same system. The former have been investigated previously using pure nuclear (electronically forbidden) reflections^{25,26} and one such effect, coherent enhancement or speedup of the time response, has been observed in previous work with this sample.^{16,27} As for the latter, we note that although the original resonant reflectivity studies using a radioactive source²⁸ were used to demonstrate interference between nuclear and electronic scattering, the mere presence of a peak at the critical angle in this work is not evidence of interference, since Eqs. (5) and (6) are insensitive to the nuclear phase (after squaring).

At grazing incidence, coherent nuclear scattering is maximized at the critical angle for external reflection. This may be explained in the context of a distorted-wave Born approximation. However, for quantitative agreement with this enriched sample, it is necessary to include higher-order terms. The presence of both strong nuclear and electronic scattering into the reflected beam is a somewhat novel situation in the context of synchrotron work. However, as the field develops, and, as new beamlines devoted to nuclear scattering become operative at third generation synchrotron facilities,²⁹ such situations will become more common. Accordingly, the enhancement of the resonant nuclear signal where the electronic scattering changes rapidly with angle will have some practical importance.

The authors would like to thank E. Alp, T. Mooney, and T. Toellner for the loan of their high-resolution monochromator crystals¹¹ and N. N. Salashchenko and S. I. Shinkarev for preparation of the sample. Support for this research was provided by the U.S. Department of Energy under Contract No. DE-AC03-76FS00515 and by the I. V. Kurchatov Institute in Moscow.

¹See R. Ruffer, *Synchrotr. Radiat. News* **5**, 25 (1992) and references therein.

²A. H. Compton, *Philos. Mag.* **45**, 1121 (1923).

³L. G. Parratt, *Phys. Rev.* **95**, 359 (1954).

⁴W. C. Marra, P. Eisenberger, and A. Y. Cho, *J. Appl. Phys.* **50**, 6927 (1979).

⁵R. S. Becker, J. A. Golovchenko, and J. R. Patel, *Phys. Rev. Lett.* **50**, 153 (1983).

⁶J. C. Frost, B. C. C. Cowie, S. N. Chapman, and J. F. Marshall, *Appl. Phys. Lett.* **47**, 581 (1985).

⁷M. A. Andreeva, G. N. Belozerskii, S. M. Irkaev, V. G. Semenov,

A. Y. Sokolov, and N. V. Shumilova, *Phys. Status Solidi A* **127**, 455 (1991).

⁸S. Isaenko, A. I. Chumakov, and S. I. Shinkarev, *Phys. Lett. A* **186**, 274 (1994).

⁹Throughout this paper, impulse excitation is assumed to take place in a time short compared to the resonant response of the system and the incident bandwidth is, correspondingly, much larger than the resonance bandwidth, but not so large as to allow significant variation in the scattering amplitude of the nonresonant background.

¹⁰G. Faigel, D. P. Siddons, J. B. Hastings, P. E. Haustein, J. R.

- Grover, J. P. Remeika, and A. S. Cooper, *Phys. Rev. Lett.* **58**, 2699 (1987).
- ¹¹T. Ishikawa, Y. Yoda, K. Izumi, C. K. Suzuki, X. W. Zhang, M. Ando, and S. Kikuta, *Rev. Sci. Instrum.* **63**, 1015 (1992).
- ¹²T. S. Toellner, T. Mooney, S. Shastri, and E. E. Alp, in *Optics for High-Brightness Synchrotron Beamlines, San Diego, California*, edited by J. Arthur, SPIE Proc. Vol. 1740 (SPIE, Bellingham, WA, 1992), pp. 218–222.
- ¹³S. Kishimoto, *Rev. Sci. Instrum.* **63**, 824 (1992).
- ¹⁴A. Q. R. Baron and S. L. Ruby, *Nucl. Instrum. Methods Phys. Res. A* **343**, 517 (1993).
- ¹⁵J. B. Hastings, D. P. Siddons, G. Faigel, L. E. Berman, P. E. Haustein, and J. R. Grover, *Phys. Rev. Lett.* **63**, 2252 (1989).
- ¹⁶A. Q. R. Baron, J. Arthur, S. L. Ruby, D. E. Brown, A. I. Chumakov, G. V. Smirnov, G. S. Brown, and N. N. Salashchenko (unpublished).
- ¹⁷S. Kikuta, in *X-ray Resonant (Anomalous) Scattering*, edited by G. Materlik, C. J. Sparks, and K. Fischer (Elsevier, Amsterdam, 1994), pp. 635–646.
- ¹⁸See, e.g., R. W. James, *The Optical Principles of the Diffraction of X-rays* (Cornell University Press, Ithaca, 1965), p. 173.
- ¹⁹Calculated based on D. T. Cromer and D. A. Liberman, *Acta Crystallogr. Sec. A* **37**, 267 (1981) using programs described in S. Brennan and P. L. Cowan, *Rev. Sci. Instrum.* **63**, 850 (1992).
- ²⁰Note that an analogous peak in the delayed intensity has been independently calculated for ⁵⁷Fe/⁵⁶Fe multilayers. L. Deak, L. Bottony, and D. L. Nagy, *Hyperfine Interact.* (to be published).
- ²¹G. H. Vineyard, *Phys. Rev. B* **26**, 4146 (1982).
- ²²J. P. Hannon, G. T. Trammell, M. Mueller, E. Gerdau, R. Rüffer, and H. Winkler, *Phys. Rev. B* **32**, 6363 (1985). An external magnetic field was applied to the layer perpendicular to the scattering plane so only $\Delta m = \pm 1$ transitions (lines 1, 3, 4, and 6 of the iron hyperfine sextet) interact with the sigma polarized synchrotron radiation.
- ²³H. Kiessig, *Ann. Phys. (Paris)* **10**, 769 (1931).
- ²⁴The Kiessig interference fringes shift the maximum in $dR^e/d\theta$ to higher angles so the first-order calculation is similarly shifted [see Eq. (5)]. In fact the complete calculation, the solid line in Fig. 3, and the data, also peak slightly above the nominal critical angle, which is defined for a semi-infinite sample. It is primarily the narrowness of the first-order calculation that makes the shift more apparent, though the time gating at $t=4$ ns is also seen, computationally, to reduce the shift.
- ²⁵U. van Bürck, G. V. Smirnov, R. L. Mössbauer, H. J. Marus, and N. A. Semioschkina, *J. Phys. C* **13**, 4511 (1980).
- ²⁶U. van Bürck, R. L. Mössbauer, E. Gerdau, R. Rüffer, R. Hollatz, G. V. Smirnov, and J. P. Hannon, *Phys. Rev. Lett.* **59**, 355 (1987).
- ²⁷Generalization from pure nuclear reflections [see Ref. 22, Eq. (20)] suggests maximum speedup should occur at zero angle. However, calculations for grazing incidence reflection in the presence of electronic scattering show maximum speedup at the critical angle. Experimentally, the speedup is seen to increase as the critical angle is approached from larger angles Ref. 16, but no measurement of the time response has yet been made below the critical angle.
- ²⁸S. Bernstein and E. C. Campbell, *Phys. Rev.* **132**, 1625 (1963).
- ²⁹These include the European Synchrotron Radiation Facility (ESRF) in France, the Advanced Photon Source (APS) in the United States, and Spring-8 in Japan.